

LRP 481/93

August 1993

**STOCHASTIC PLASMA HEATING BY  
ELECTROSTATIC WAVES:  
A COMPARISON BETWEEN A  
PARTICLE - IN-CELL SIMULATION AND A  
LABORATORY EXPERIMENT**

M. Fivaz, A. Fasoli, K. Appert, F. Skiff,  
T.M. Tran and M.Q. Tran

submitted for publication in

Physics Letters A

# **Stochastic Plasma Heating By Electrostatic Waves: A Comparison Between a Particle-In-Cell Simulation and a Laboratory Experiment.**

M.Fivaz, A.Fasoli, K.Appert, F.Skiff\*, T.M.Tran and M.Q.Tran

Centre de Recherches en Physique des Plasmas,  
Association Euratom-Confédération Suisse,  
Ecole Polytechnique Fédérale de Lausanne,  
21, av. des Bains, CH-1007 Lausanne, Switzerland

## **Abstract**

Dynamical chaos is produced by the interaction between plasma particles and two electrostatic waves. Experiments performed in a linear magnetized plasma and a 1D particle-in-cell simulation agree qualitatively: above a threshold wave amplitude, ion stochastic diffusion and heating occur on a fast time scale. Self-consistency appears to limit the extent of the heating process.

\*Permanent address : Laboratory for Plasma Research, Univ. of Maryland-College Park, USA.

It has been shown, both theoretically [1] and experimentally [2], that two waves propagating in a plasma can produce dynamical chaos in particle orbits. Existing theories are mainly based on the Hamiltonian single-particle approach [3], in which the response of single particles to an external field is studied. However, in real plasmas, charged particles are the sources of the internal electromagnetic fields, which, in turn, determine the motion of the particles. Self-consistency, i.e. the mutual link between fields and particles, is therefore associated with all wave-particle interaction phenomena in plasmas.

In addition, the plasma response to an external perturbation is in general non-linear, especially when high amplitude waves are employed to produce secular perturbations of the particle distribution and when resonant particles are involved, e.g. in the case of heating and non-inductive current drive in fusion oriented plasma devices [4].

Self-consistency and non-linearity cannot be treated in general terms by the existing theories. This motivates research on both simple, well-diagnosed laboratory experiments and self-consistent simulations. Specific aspects of the dynamical behavior of the wave-plasma system may be revealed by a comparative analysis of the results obtained in the two approaches. This Letter reports such a comparison, established specifically between a Q-machine linear magnetized plasma experiment and a 1-D Particle-in-Cell (PIC) simulation [5].

A self-limitation in the chaotic heating process is suggested by the experimental results [2]. The mechanisms leading to such a saturation are investigated in the simulation.

We note that in many wave-particle scenarios, both in laboratory and space plasma environments, the interaction lasts for a finite time and often occurs in a limited spatial extension. This motivates the study of the transient plasma response.

The experimental investigation is conducted on a uniform, linear magnetized Q-plasma (the "LMP" [6]). A low level of fluctuations ( $\delta n/n < 1\%$ ) and a supersonic drift along the magnetic field lines characterize the unperturbed plasma. Electrostatic waves at an angular frequency  $\omega$  in the range  $\omega_{ci} < \omega < 2\omega_{ci}$  ( $\omega_{ci}$  being the ion cyclotron frequency) are excited by a four ring antenna encircling the plasma column and electrically insulated from it. Laser Induced Fluorescence (LIF) [7] and Optical Tagging (OT) [8] provide information regarding the ion dynamical response. Time and space resolutions of these diagnostic methods are such that the details of the plasma response can be investigated locally in the space-time wave pattern. The background plasma parameters are, in terms of density, electron and ion temperatures and drift velocity:  $n_0 \approx 10^{16} \text{ m}^{-3}$ ,  $T_e \approx 2T_i = 0.2 \text{ eV}$  and  $v_D \approx 10^3 \text{ m/s}$ .

The excited waves are characterized in the direction parallel to the magnetic field by two components propagating at two different phase velocities,  $v_{\phi 1}$  and  $v_{\phi 2}$ . Experimental measurements show that the values of the two phase velocities in the plasma frame of reference are

$$v_{\phi 1} \approx -v_{\phi 2} \approx c_s = \sqrt{k_B \frac{T_e + 3T_i}{m_i}}$$

in agreement with the ion acoustic wave dispersion relation for long wavelength. The difference in phase velocity,  $\Delta v_\phi = v_{\phi 1} - v_{\phi 2}$ , is of the order of the plasma drift velocity and allows one to neglect, to a first approximation, the multiple island structure produced over the ion phase space by the non-zero perpendicular wave numbers [9]. A one-dimensional representation of an unmagnetized plasma with two ion-acoustic propagating waves, corresponding to the parallel direction, is therefore expected to describe the principal physical properties of the interaction of particles with two waves.

Such a representation is provided by a fully self-consistent particle-in-cell simulation, which inherently includes the feedback action of modified particle orbits on the plasma wave fields, wave non-linearity and damping. A modified version of the 1-D particle-in-cell code XES1 [5] has been used. Whilst ions are represented by particles, a Boltzmann density distribution is assumed for electrons at thermal equilibrium

$$n_e = n_0 \exp\left(\frac{e \phi}{k_B T_e}\right) \quad (1)$$

where  $k_B$  is the Boltzmann constant,  $\phi$  the wave electric potential. Since the wavelengths considered are much longer than the electronic Debye length, the quasi-neutrality condition  $n_i = n_e$  is used to calculate the electric potential [10].

Periodic boundary conditions are imposed, with a period larger than the extension of the observed space, which in turn exceeds by more than an order of magnitude the typical wavelengths. Spatial filtering is

used [5] to avoid short wavelength numerical noise and to reduce wave non-linearities at large wave amplitudes ( $\delta n/n > 50\%$ ), consistent with the experimental observations. The initial ion velocity distribution is a non-drifting Maxwellian. Second-order splines are used for the charge assignment and the scheme is energy-conserving. This model is able to simulate a fully self-consistent, low frequency wave-plasma system in the Vlasov approximation, and to reproduce in particular the complex ion acoustic dispersion relation.

The simulation is performed in the plasma reference frame. The antenna is simulated by adding to the potential  $\phi$  the quantity

$$\phi_a(x,t) = A_a \exp\left(-\left(\frac{x-x_a(t)}{\delta_a}\right)^2\right) \sin\left(2\pi \frac{x-x_a(t)}{\lambda_a}\right) \sin(\omega_a t) \quad (2)$$

with  $x_a(t) = x_0 + V_D t$  and where  $\delta_a$ ,  $\lambda_a$ ,  $x_0$ ,  $V_D$  and  $\omega_a$  are, respectively, spatial extension, characteristic wavelength, initial position, velocity and angular frequency of the antenna,  $A_a$  the excitation amplitude and  $x$  the spatial coordinate. The antenna velocity  $V_D$  represents the plasma drift characterizing the LMP experiment.

The antenna velocity is set approximately equal to twice the phase velocity. In this particular case, the induced waves, propagating in opposite directions, are characterized by Doppler-shifted angular frequencies of about  $\omega_a$  and  $\omega_a/3$ . The coupling efficiency of the two modes depends upon plasma and antenna parameters and decreases at high excitation regimes. At very large amplitude, it is observed that the antenna does not generate propagating waves, but reflects bursts of ions. The density is consequently reduced behind the antenna. Both

effects are indeed observed in the LMP experiment, where ballistic-like disturbances propagating upstream with respect to the ring antenna are clearly identified on the ion distribution [11].

In the simulation, to overcome the difficulty of launching simultaneously the two modes at high amplitude, we use two antennas at different locations. The parameters  $\delta_a$  and  $\lambda_a$  are chosen to maximize the coupling with the mode propagating in the antenna direction at frequency  $\omega_a$ . The second mode has very low amplitude ( $\delta n/n < 1\%$ ) and is masked by the noise.

The two antennas are turned on at  $t=0$  (Fig. 1a) with opposite velocities ( $V_D$  and  $-V_D$ ) and opposite amplitudes ( $A_a$  and  $-A_a$ ). They are turned off when they meet (Fig. 1b). The two wave packets generated cross each other, interacting during a finite time. The ion temperature is measured in the region of interaction once the wave packets have separated (Fig. 1c). The temperature measurement is therefore not affected by the direct perturbation of the velocity distribution due to the large amplitude waves.

The two ion-acoustic wave packets have opposite phase velocities  $c_s$  and  $-c_s$ . Their difference in phase velocity is  $2 c_s$  and is equal to the antenna velocity. The conditions of the experiment are therefore reproduced in this respect.

According to the Chirikov criterion [12], when the wave amplitude is such that the separatrices associated with the two primary islands begin to overlap, the onset of stochastic-like orbits triggers a sudden

transition in the phase space topology. Macroscopically, rapid plasma heating is produced.

The transition wave amplitude can be quantified by introducing the stochasticity parameter  $K$  [1]

$$K = 2 (A_1^{1/2} + A_2^{1/2}) \quad (3)$$

where  $A_i = \frac{e\phi_i}{m(\Delta v_\phi)^2}$  is the normalized amplitude of the mode  $i$  ( $i=1,2$ ).

Dynamical chaos is expected to occur for  $K \geq 1$ .

First, we consider a non-self-consistent one-particle model. In this case, one integrates the orbits of non-interacting particles in the field of an antenna-generated electrostatic wave. This is obtained by separating the ions into two sets [5]:

Firstly, a zero-temperature set containing one particle only at the center of each cell. To each particle is attributed 0.1% of the normal charge-over-mass ratio. These particles are therefore maintained near their initial position and thus respond linearly to any external field, and form the dielectric medium necessary for the wave propagation.

Secondly, a set of test particles with Maxwellian initial velocity distribution. These test particles are given negligible density. They have therefore negligible influence on the field and do not interact with each other. All particle measurements are performed on this group.

Despite its non-self-consistent nature, this model can highlight the paradigm of the wave-induced ion stochastic diffusion in velocity



space, establishing a link between previous single particle Hamiltonian models and the fully self-consistent simulations described below.

Figure 2 shows the ion phase space at two successive times, during the two-wave particle interaction with an excitation amplitude such that  $K > 1$ . Within a few wave periods, test particle orbits undergo a transition from regular to chaotic. This transition does not occur if one antenna only is used, in which case the particle orbits are integrable. It does not occur either at excitation amplitude such that  $K < 1$ , as the particle orbits are quasi-integrable even in the presence of two waves, in the sense that most regular surfaces are conserved. These results are in agreement with previous Hamiltonian single particle analyses [3]. The outermost regular KAM surfaces [13] limit the particle excursion in phase space, preventing the occurrence of large scale chaotic diffusion.

Note that a direct estimation of the kinetic temperature in the strong excitation regime would be affected by the coherent wave perturbation on the ion distribution, especially at the low ion temperatures used in the simulations.

We now consider the fully self-consistent particle-in-cell simulations. For  $K > 1$ , the orbits observed in phase space do not undergo as clear a change in their character. However, a significant increase in temperature, indicating stochastic diffusion, is measured at high excitation amplitude.

The temperatures measured in the experiment and in the simulations are shown as a function of the excitation amplitude in Figure 3. More

specifically, Figure 3a shows the final ion temperature measured in the simulation, in the configuration described earlier, whilst the experimental data reported in Figure 3b refer to the direct observation of the parallel ion distribution via LIF. The two curves indicate a significant heating for amplitudes exceeding a certain threshold value.

The wave amplitude can be calibrated via the ion dielectric response [14] in the experiment, and through direct potential measurements in the simulation. The value of the stochasticity parameter  $K$  can then be calculated. The shaded areas on the amplitude axis of the two graphs correspond to  $K=1$  (eq. 3) within the uncertainty of the measurements. Both experiment and simulation are found to agree with the analytical prediction on the value of the threshold wave amplitude.

In the simulations, the effects of the interaction of particles with two waves can be isolated from those due to the interaction of the plasma with one wave or with the local antenna potential. This is achieved by running a second set of simulations with the same parameters, but one antenna only. The heating appears exclusively in the two antenna case (Figure 3a). The two-wave particle interaction is therefore responsible for the observed heating.

In the experiment, the time scale for the heating process can be evaluated by gating the wave generator and observing the ion distribution as a function of time from the beginning of the excitation. Correspondingly, in the simulation, the time scale is estimated by varying the duration of the excitation (and selecting an initial antenna separation accordingly), thereby varying the time during which the plasma is subjected to the action of the two waves.

The temporal evolution of the local ion temperature obtained from the simulation and the LMP experiment are displayed in Figure 4. The excitation amplitude is above the threshold appearing on Figure 3. A linear increase of  $T_i$ , indicating a diffusive process, is obtained in both cases. An estimate of the velocity space diffusion coefficient averaged over all velocity classes can be obtained from the slope of these curves; although not directly comparable, the values resulting from the experiment and the simulation are of the same order of magnitude. A qualitative agreement is found with the predictions based on a quasi-linear formalism [9] and, more importantly, the absolute values are more than an order of magnitude larger than those due to collisional processes [15].

Dynamical chaos in ion orbits therefore appears as the mechanism responsible for the observed heating via electrostatic plasma waves. In the same kind of experiment, a test-particle phase space transport measurement (via OT) has also indicated an exponential separation of initially-close ion trajectories [2], confirming the chaotic character of the ion response to two large amplitude waves, namely the local instability with respect to initial conditions [16].

In addition, experiment and simulation are characterized by a saturation in time of the heating process. An indication regarding the saturation mechanism is obtained in the simulation, which shows an enhancement in the wave damping during the particle stochastic diffusion.

In the experiment, the wave amplitude depends linearly on the excitation amplitude for all the points displayed in the figure 3b,

whilst in the simulation, a saturation of the wave amplitude is observed at an excitation amplitude of  $A_a \approx 0.1$  eV, corresponding to the above-mentioned limit above which propagating waves cannot be generated. The final temperature cannot be increased (Fig. 3a) above this value. On the experimental side, an analogous saturation in the dependence of the velocity space diffusion coefficient on the excitation amplitude has been identified [2]. Self-consistency therefore appears to limit the phase space stochastic transport. Chaos seems to be self-limited in actual antenna driven wave-particle systems.

The non-linear character of the high amplitude ( $K > 1$ ) waves in the simulation is shown in Figure 5, which displays the electric potential and the phase space of a typical wave packet. A non-monochromatic wave number spectrum characterizes the excited modes in the strong excitation regime. This appears to be different in the LMP experiment, as observations of the density oscillation frequency spectrum, the ion dielectric response and the spatial wave patterns do not show a strongly non-linear wave behavior up to amplitudes above the stochastic thresholds. The LMP is in fact characterized by a cylindrical symmetry, with the symmetry axis coinciding with the direction of the static magnetic field lines. This difference of geometry can account for the observed disagreement with the simulation results in two ways:

Firstly, the ion acoustic waves propagate without dispersion along the magnetic field in the experiment as well as in the 1D simulation model because the excited wavelength are much larger than Debye length. This fact favors wave steepening [17]. The experimentally

excited waves exhibit, however, a perpendicular structure with  $k_{\perp} \rho_i \approx 0.5 - 1.0$  (where  $\rho_i$  is the ion Larmor radius) hindering the formation of aligned resonant wave triplets and hence wave steepening.

Secondly, the parallel phase space of a magnetized 2-D plasma is characterized by a series of cyclotron resonances [18]. The threshold for the transition to dynamical chaos is therefore lower than in the 1-D case. Furthermore, both the principal and the cyclotron resonances will be broadened in parallel phase space by any dispersion in the wave vector direction, facilitating once again the transition to a chaotic ion response with respect to the pure one-dimensional case.

The ion temperature at saturation is lower in the simulation than in the LMP experiment and depends weakly (much slower than linearly) on the initial temperature. In order to clearly demonstrate the heating effect, the initial ion temperature was set at a value of 0.004 eV, much below the experimental value.

The simulations show non-linear wave-wave interaction, as the superposition of the two wave packets produces lower absolute values of the electric potential perturbation (typically 20% less) than a linear superposition. This can account in part for the lower final temperature.

In summary, two high amplitude ion-acoustic waves excited by an antenna in a drifting plasma and propagating with two different phase velocities have been shown to generate stochastic plasma heating, both in a particle simulation and in a linear magnetized plasma experiment. The existence of a threshold wave amplitude and velocity space fast diffusion above threshold have been demonstrated in both cases. In

particular, heating of the plasma bulk with a temperature enhancement of a factor larger than five is observed.

Stochastic heating and diffusion are partly limited by wave-wave non linearities and by the finite interaction time set by an enhanced wave damping. Self-consistent effects also limit the amplitude of the antenna excited modes and modify the wave spectrum. More restrictive conditions than those predicted by the standard Hamiltonian single particle models for the occurrence of the heating process are therefore suggested.

This work was partly supported by the Swiss National Science Foundation. We thank C.K. Birdsall for useful discussions and for letting us use the XGRAFIX package. We are also grateful to T. Gunzinger for letting us perform part of the simulations on the MUSIC parallel machine.

## References

- [1] D.F. Escande, *Phys. Rep.* **121**, 166 (1985)
- [2] A. Fasoli, F. Skiff, R. Kleiber, M.Q. Tran and J.P. Paris, *Phys. Rev. Lett.* **70**, 303 (1993)
- [3] "Intrinsic Stochasticity in Plasmas", edited by G. Laval and D.Grésillon, Editions de Physique, Orsay 1979
- [4] K. Miyamoto: "Plasma Physics for Nuclear Fusion", *MIT Press*, Cambridge (1980)
- [5] C.K. Birdsall & A.B. Langdon: "Plasma physics via computer simulation", *Adam Hilger*, Philadelphia (1991)
- [6] P.J. Paris and N.Rynn, *Rev. Sci. Instrum.* **61**, 1096 (1990)
- [7] R.A. Stern, D.N.Hill and N.Rynn, *Phys. Rev. Lett.* **37**, 833 (1981)
- [8] R.A. Stern, D.N.Hill, and N.Rynn, *Phys. Lett.* **93A**, 127 (1983)
- [9] R.Z. Sagdeev, D.A.Usikov, G.M.Zaslavsky, *Nonlinear Physics*, Harwood Academic Publishers, Chur (1988)
- [10] T. Tajima, "Computational Plasma Physics", *Addison-Wesley*, New-York (1989)
- [11] A. Fasoli, Ph.D. Thesis n. 1162, *EPFL*, Lausanne (1993).
- [12] B.V. Chirikov, *Phys. Rep.* **52**, 263 (1979)
- [13] "Ergodic Problems in Classical Mechanics", edited by V.I.Arnold and A.Avez, *Benjamin*, New York (1968)
- [14] F. Skiff and F.Anderegg, *Phys. Rev. Lett.* **59**, 896 (1987)
- [15] J. Bowles, R.Mc Williams, and N. Rynn, *Phys. Rev. Lett.* **68**, 1144 (1992)

- [16] A.J. Lichtenberg, "Regular and Stochastic Motion", *Springer-Verlag*, New York (1983)
- [17] B.B Kadomtsev, "Phénomènes collectifs dans les plasmas", *Ed. mir*, Moscow (1979)
- [18] G.R. Smith and A.N.Kaufman, *Phys. Rev. Lett.* **34**, 1613 (1975)



## Figure Captions

**Figure 1.** Sketch of the simulation procedure. The excitation is started at  $t=0$  (a) and stopped once the antennas begin to overlap (b). The ion temperature is measured in the black region when the two generated wave packets have crossed each other (c).

**Figure 2.** One-particle simulation: snapshots in time of the ion phase space at the beginning of the two wave - particle interaction (a) and after 5 wave periods (b). Trapped and non trapped particles are visible in the potential structure at both sides of the first graph.

Here and in the following figures,  $V_a = \pm 1.05 \cdot 10^3$  m/s,  $\omega_a = 3.5 \cdot 10^6$  rad/s,  $\delta_a = 6.2 \cdot 10^{-4}$  m and  $\lambda_a = 9.3 \cdot 10^{-4}$  m,  $T_e = 0.4$  eV and  $n_0 = 10^{16}$  m $^{-3}$ . The initial ion temperature is  $T_i = 0.0036$  eV. Here and in Fig. 5 the spatial positions are normalized to the cell length,  $dx = 4.88 \cdot 10^{-5}$  m.

**Figure 3.** (a) PIC simulation: final temperature as a function of excitation amplitude for the normal, two-antenna set-up (solid dots) and with one antenna only (open dots). The excitation duration is 8 antenna periods. A spatial filter of shape function  $\exp(-k^2/k_0^2)$  is applied on Fourier transformed electric potential, with  $k_0 = 6.28 \cdot 10^4$  m $^{-1}$  in all simulations.

(b) LMP experimental results: LIF measured parallel steady state ion temperature as a function of the excitation amplitude. The antenna angular frequency is 157 KHz.

The ion temperature is measured by fitting (minimizing the integral of the square difference) a Maxwellian to the measured distribution function.

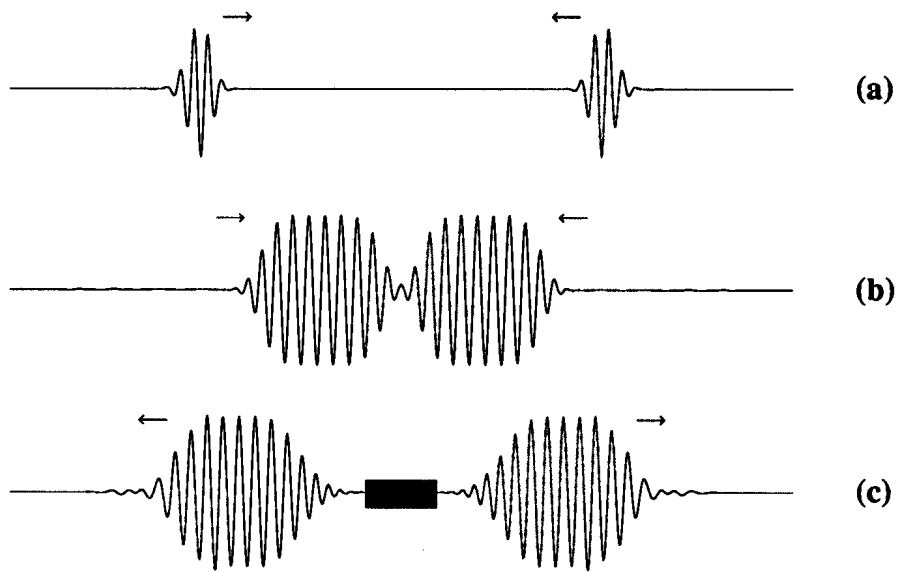
The shaded area corresponds to  $K=1$  (eq. 3).

**Figure 4.** Final temperature in PIC simulation (a) for the normal, two-antenna set-up (solid dots) and with one antenna only (open dots), and time-resolved parallel temperature in the LMP experiment (b) as a function of the interaction time, expressed in units of the antenna period.

Excitation amplitude is fixed above threshold ( $K>1$ ).

**Figure 5.** PIC simulation: detail of (a) the electric potential and (b) the ion phase space for a wave packet with an amplitude above threshold ( $K>1$ ).

**Figure 1**



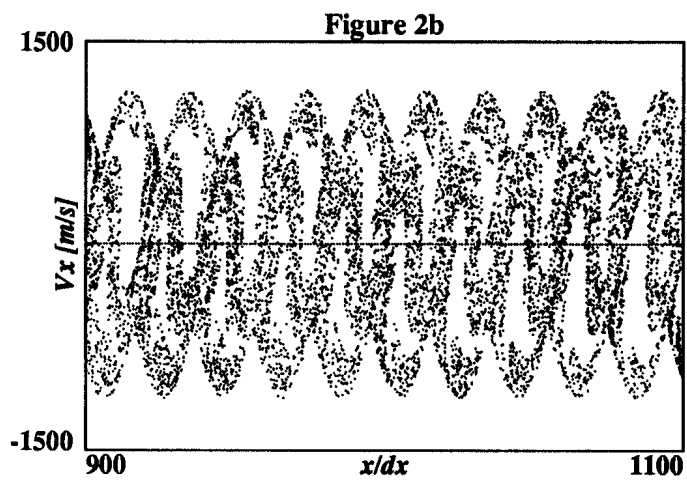
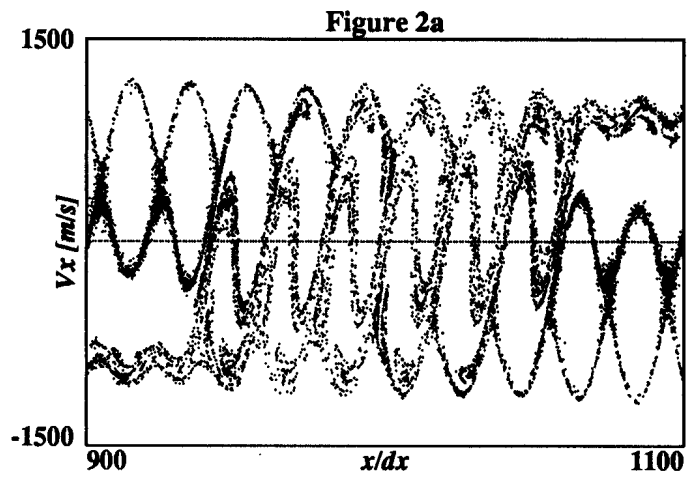


Figure 3a

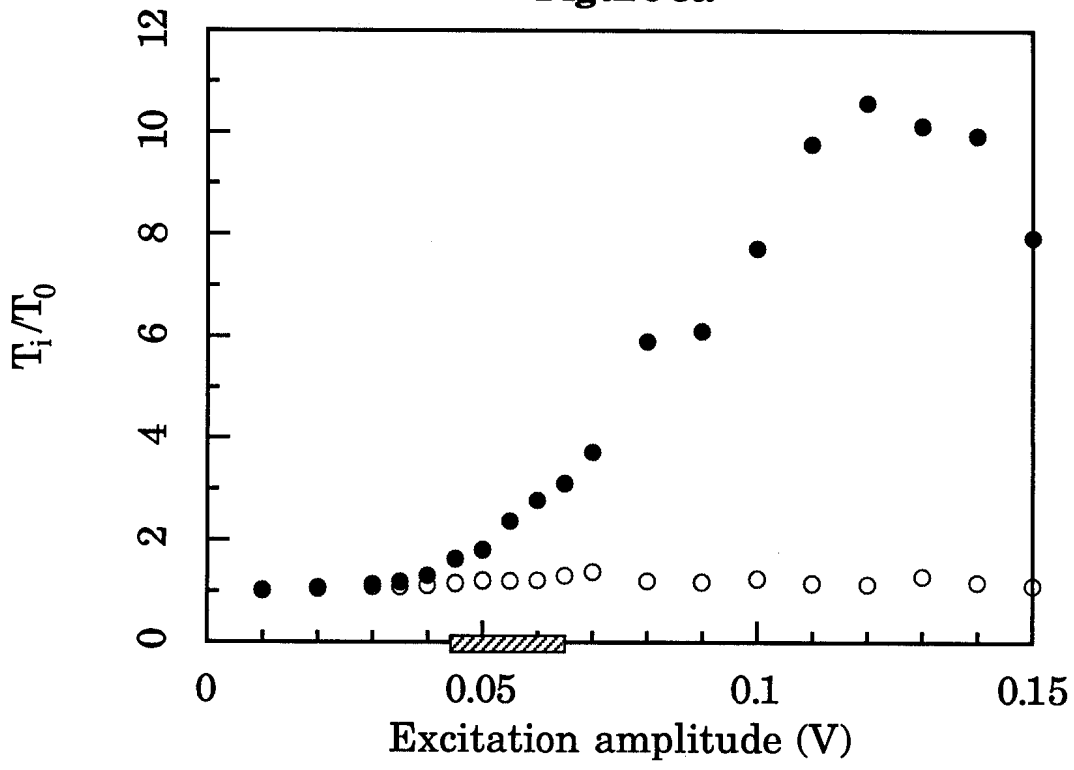


Figure 3b

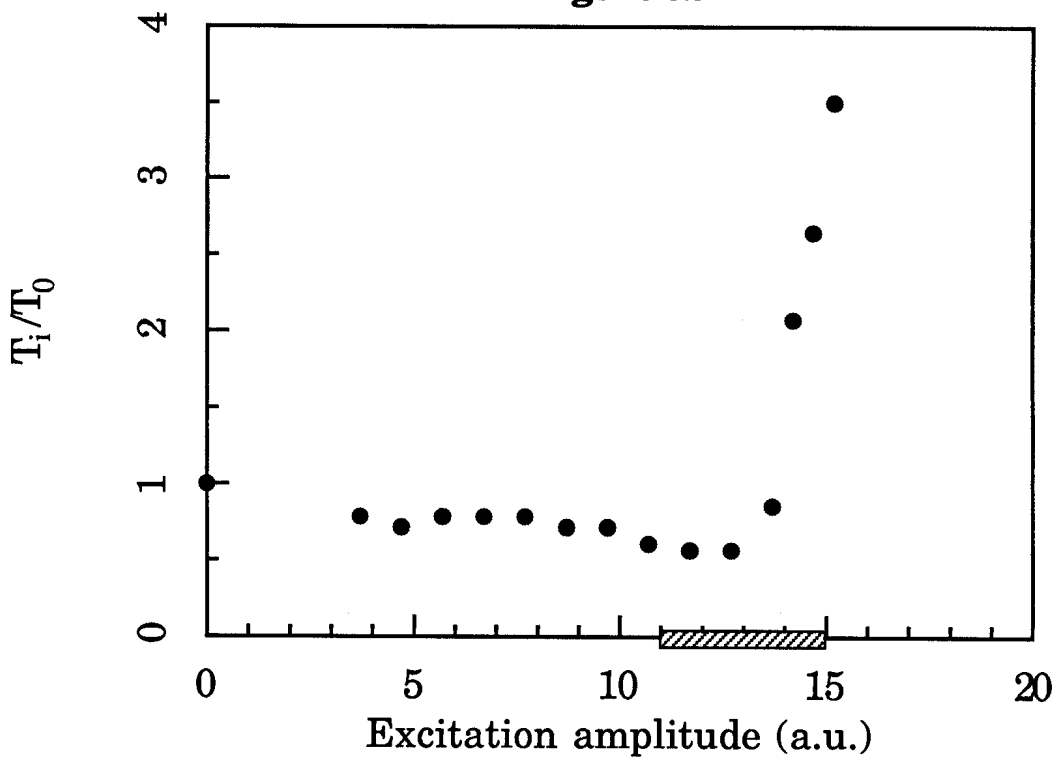


Figure 4a

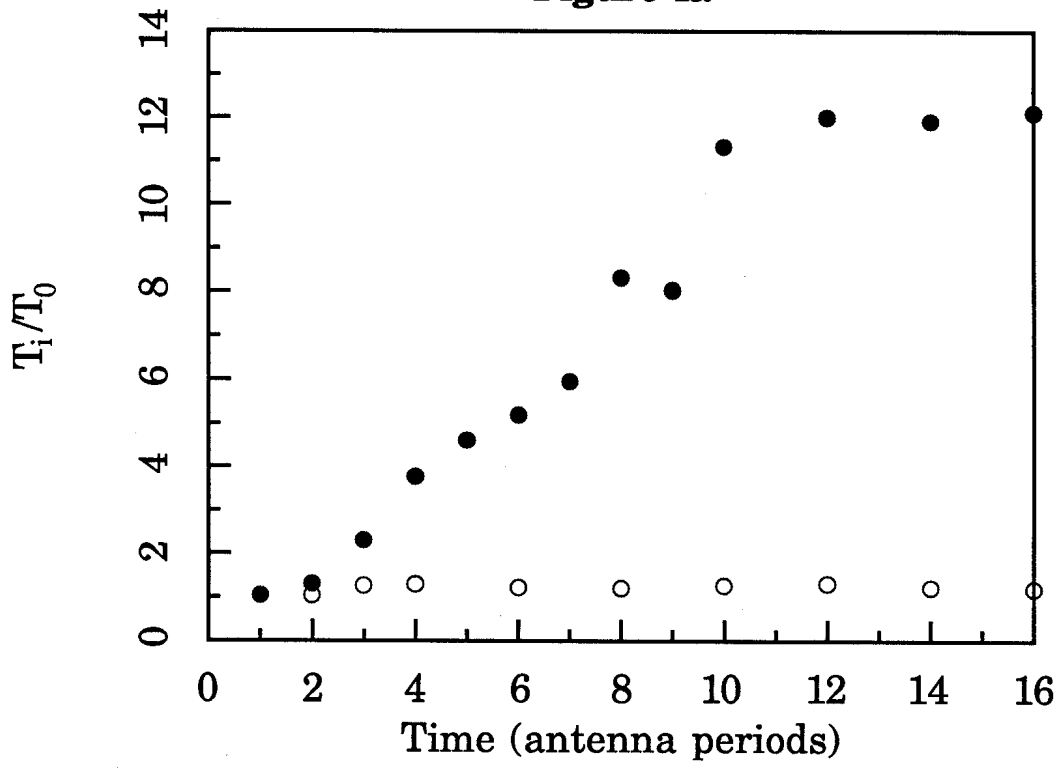
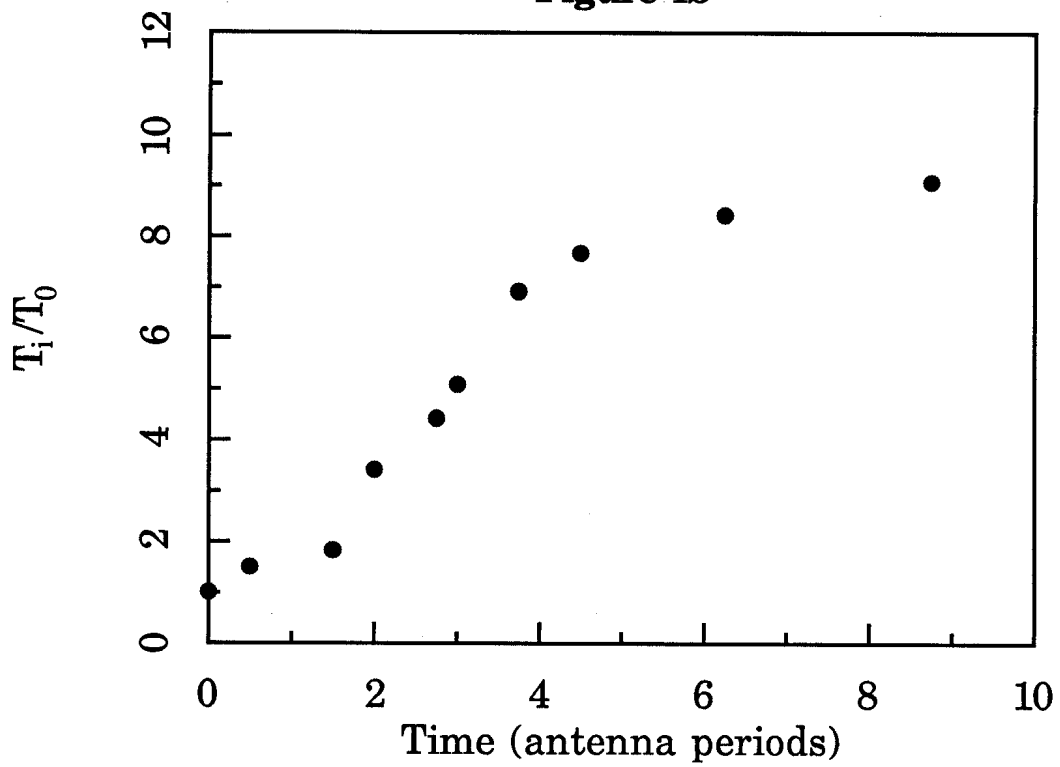
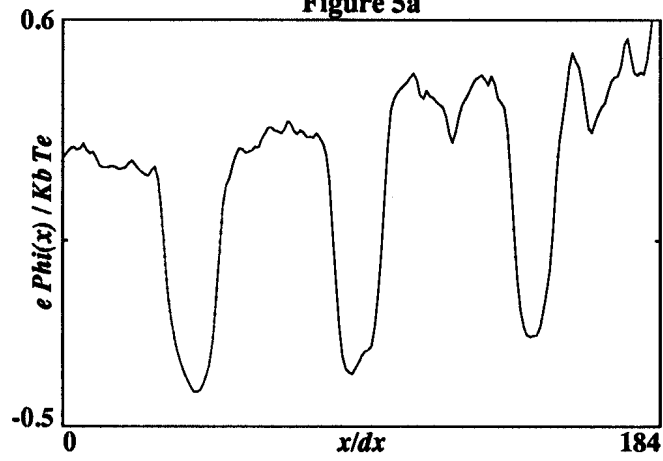


Figure 4b



**Figure 5a**



**Figure 5b**

